Structural Concepts for Future Space Transportation System Orbiters

Allan H. Taylor,* L. Robert Jackson,† and Randall C. Davis,†
NASA Langley Research Center, Hampton, Virginia
and
Jeffrey A. Cerro‡ and Stephen J. Scotti‡
Kentron International Inc., Hampton, Virginia

Future Space Transportation Systems (FSTS) are being studied to identify critical technology needs for timely development of FSTS with the following goals: 150,000-lb payload, long life, fully reusable, all-weather operational capability, and durable structures and systems to minimize refurbishment, maintenance, and cost.

Two structural concepts for the FSTS second-stage orbiter were analyzed considering cyclic life, fracture mechanics, thermo-structural and aerodynamic thrust loads, propellant compatibility and operational flexibility. These two orbiter concepts were compared on the basis of weight and ability to meet structural goals. The first concept involves only incremental advancements over current structural technology. The second concept involves more advanced structural technology. The first concept has two blade-stiffened aluminum cryogenic tanks suspended within an insulated aluminum airframe structure. The advanced concept has a blade-stiffened aluminum tank/thrust structure supporting a hot advanced carbon-carbon (ACC) aeroshell structure. The weight advantage and potential for meeting the structural goals make the advanced concept attractive for FSTS consideration.

Nomenclature

E = modulus of elasticity, lb/in.^{2}
g = acceleration due to gravity, ft/s^2
l = length, in.
K_I = stress intensity factor
M = Mach number
N = load intensity, lb/in.
R = radius, in.
$\bar{t}$ = equivalent thickness, in.

Subscripts

x = axial direction
y = lateral direction
z = normal direction

Abbreviations

ACC = Advanced Carbon Carbon
GLOW = Gross Lift-Off Weight
FSTS = Future Space Transportation Systems
LH_2 = Liquid Hydrogen
LOX = Liquid Oxygen

Introduction

PREVIOUS studies[1-3] have identified economic advantages of fully reusable space transportation systems. These studies show that the cost-effectiveness of this class of vehicles is largely dependent on the mass-strength efficiency and durability of the structure. Future space transportation systems for the post-Shuttle time frame are being studied. An objective of this study is to identify critical technology requirements for the timely development of such a vehicle. A two-stage, vertical takeoff, fully reusable, all-rocket system was used for the present technology study considering the system and structural goals shown in Fig. 1. This study considered the usual disciplines of propulsion, performance, aerodynamics, structures and materials. In addition, the influence of such factors as operations, mission analysis, manufacturing, maintainability, and cost on the mission goals are considered in this study.

This paper describes two structural concepts for an orbiter vehicle and presents the results of an analysis of the ability of these two concepts to meet structural goals. The two basic structural concepts considered were a near-art concept, using incremental advances over current technology, and an advanced technology concept. The near-art concept is an insulated aluminum airframe similar to the current Space Shuttle which carries on-board cryogenic propellants in nonintegral tanks. This concept will require minimal development and can easily meet a 2005 date for initial operations capability. The advanced technology concept is an integral tank/thrust structure of aluminum alloy supporting a separate aeroshell hot structure of advanced carbon-carbon. The carbon-carbon hot structure carries the aerodynamic loads and protects the inner tank/thrust structure. This concept requires further development to meet the 2005 operational date. Both concepts were analyzed using loads obtained from

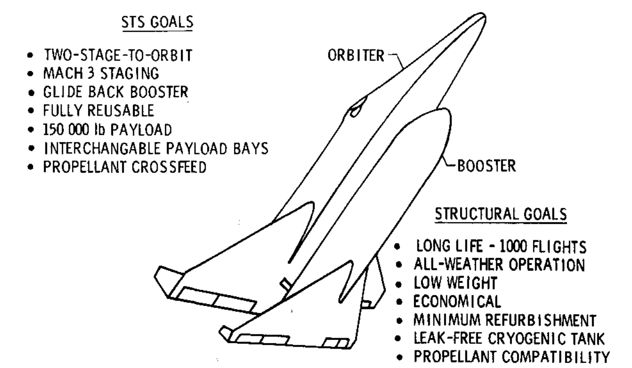

Fig. 1 Two stage-to-orbit, fully reusable space transportation system.

Presented as Paper 83-0210 at the AIAA 21st Aerospace Sciences Meeting, Reno, Nev., Jan. 10-13, 1983; received Jan. 24, 1983; revision received June 5, 1984.

*Aerospace Engineer. Associate Fellow AIAA.
†Aerospace Engineer.
‡Senior Structures Engineer. Member AIAA.

optimum flight trajectories and compared for their ability to satisfy structural goals.

Vehicle Description

The FSTS configuration shown in Fig. 1 is a two-stage, fully reusable system concept for inserting a 150,000-lb payload into a 262 n.m. near-Earth orbit at 31 deg inclination. The gross lift-off weight is approximately 5.4 million lb. The weight of the orbiter alone is 3 million lb. The orbiter is rocket-propelled using modified shuttle main engines with liquid oxygen and liquid hydrogen propellants. The booster is powered by a gas generator hydrocarbon rocket engine. The mated booster and orbiter are vertically launched with the booster cross-feeding propellants to the orbiter until staging at Mach 3. After staging, the booster glides back to the launch site, while the fully fueled orbiter continues the mission to orbit and returns for a horizontal landing similar to the current Space Shuttle.

The general arrangement for the orbiter, shown in Fig. 2, was initially sized for the structural concept of Ref. 1 using the method of Ref. 4. The vehicle is approximately 200 ft long, 34 ft high and as a 45 deg swept wing with a span of 150 ft. The maximum wing thickness is 12% of the chord, the wing reference area is 7000 sq ft.[2] The propellants are contained in twin-lobed tanks within a D-shaped fuselage which is about 50 ft wide. The forward tank contains 340,000 lb of LH_2, while the smaller aft tank holds 2.0 million lb of LOX. Approximately 80% of the orbiter lift-off mass consists of expendable propellants.

Structural Concepts

Near-Art Concept

The near-art concept is shown in Figs. 3 and 4. The structural arrangement, Fig. 3, is an insulated, aluminum skin-stringer airframe with nonintegral propellant tanks suspended within the airframe by ball-jointed links to accommodate differential thermal growth while transmitting inertial loads. The airframe wall construction, shown in Fig. 4, consists of an aluminum skin with capped sine-wave web stringers and ring frames. The rocket thrust is carried into the airframe via an integral thrust structure bulkhead consisting of a grid of beams. A mechanically attached durable thermal protection system[5] consists of 12 in. × 12 in. metallic and 36 in. × 36 in. carbon-carbon packages (tiles) containing fibrous insulations. The nonintegral welded aluminum, blade-stiffened skin tanks are insulated with reinforced closed-cell foam insulation (internal and external) for the LH_2 and LOX tanks, respectively) similar to the Saturn S-IVB stage. The foam is external on the LOX tank because the organic based foam is LOX-sensitive (that is, with little ignition energy, it burns in the presence of LOX). The foam insulation is required to prevent air liquefaction and with a heated dry air (or possible nitrogen) purge, maintains a relatively warm aerodynamic surface temperature to prevent frost (from humidity) or ice (from rain) buildup on the orbiter surface or between the TPS tiles. The durable TPS is sized to keep the aluminum structure below 350°F and the internal cryogenic foam below 175°C throughout the mission.

Advanced Concept

Figures 5 and 6 depict the advanced technology concept. A novel dual structural arrangement is used for the orbiter consisting of a tank/thrust structure within airframe structure or aeroshell. The tank/thrust structure consists of cryogenic propellant tanks with integral thrust structure. The tank/thrust structure is supported by aft trunnion and forward hinged supports within the aeroshell which accommodate thermal growth while transmitting inertial loads. The rocket thrust is connected directly to the tank structure providing a short load path between the engines and propellant mass. This load path results in a more highly loaded tank/thrust structure than the near-art nonintegral tanks but results in a lightly loaded aeroshell structure since the normal accelerations or lift forces are relatively low for vertical takeoff vehicles. The tank/thrust structure can be removed for inspection and maintenance by

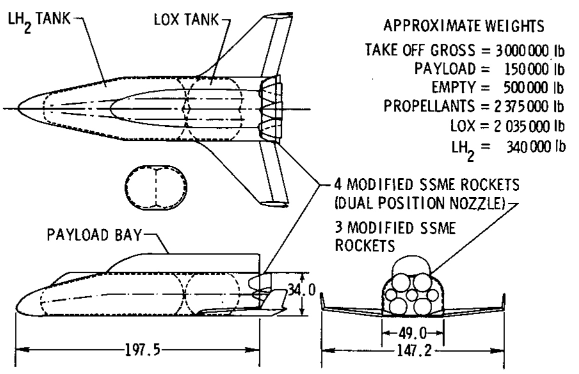

Fig. 2 General arrangement FSTS orbiter (dimensions in ft).

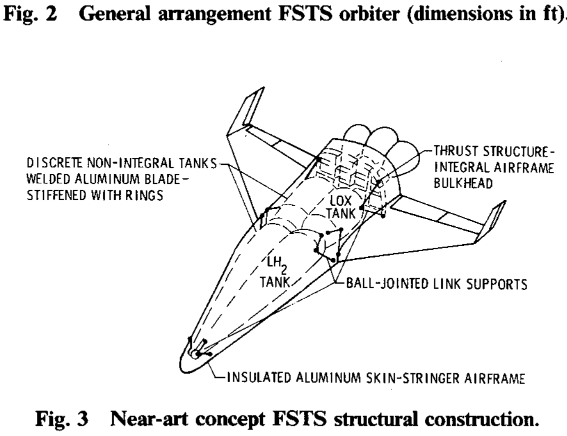

Fig. 3 Near-art concept FSTS structural construction.

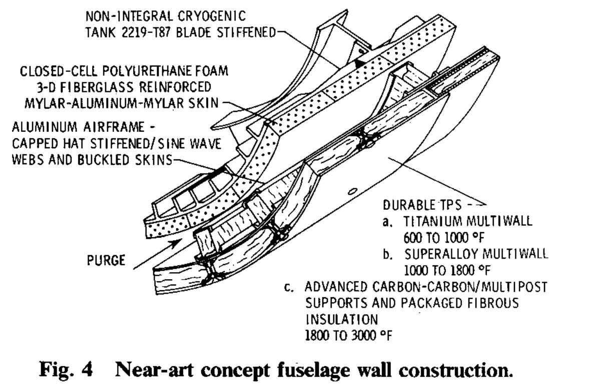

Fig. 4 Near-art concept fuselage wall construction.

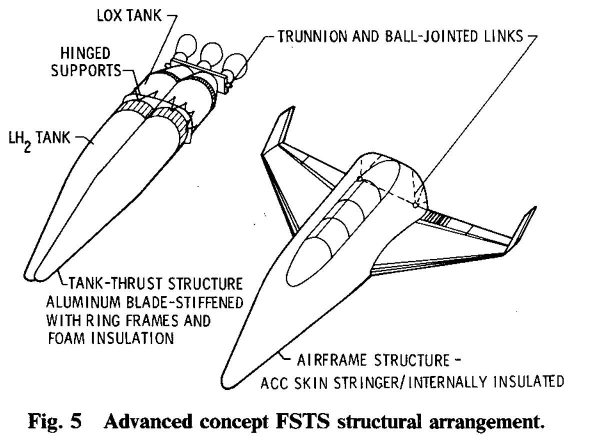

Fig. 5 Advanced concept FSTS structural arrangement.

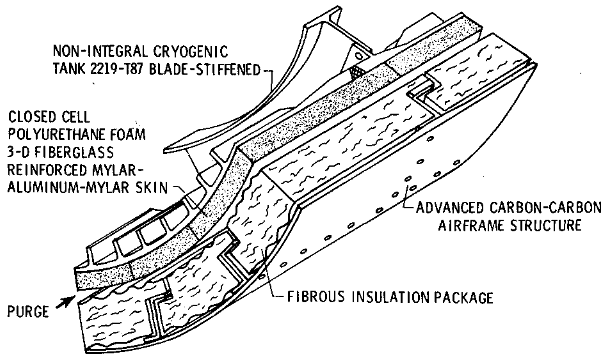

Fig. 6 Advanced concept fuselage wall construction.

disconnecting attachments between the structures and sliding the aeroshell forward with respect to the tank-thrust structure.

The wall construction of the aeroshell orbiter fuselage is shown in Fig. 6. The cryogenic tanks are similar to the near-art concept, but the aeroshell, a hot structure which carries the aerodynamic loads, is fabricated from advanced carbon-carbon similar to the ACC material described in Ref. 6. The ACC aeroshell requires no external TPS; however, packaged fibrous insulation (microquartz, contained in a foil-gage nickel-alloy package) is required between the hot ACC aeroshell and the outer tank wall to limit the temperatures of the aluminum tank or cryogenic foam. The space between the tank/thrust structure and the aeroshell structure is purged during periods of ground hold with a heated purge gas, similar to the near-art concept.

Trajectories

The nominal ascent and entry trajectories used for this study were obtained from a trajectory optimization program[7] using a 3 g axial acceleration limit and a normal acceleration limit of 2.5 g during entry and 0.48 g during ascent. The latter limit was imposed on the ascent trajectory so that the wing loading with propellants on board does not exceed the wing loading with tanks empty during entry. The booster separates from the fully fueled orbiter at Mach 3 approximately 110 s into the flight.

Loads, Design Criteria, and Bending Moments

Loads

The flight trajectories are used to calculate structural loads and determine the aerodynamic heating rates. The orbiter was assumed to have no loads applied by the booster when mated. The maximum structural loading occurs when an axial acceleration of 2.2 g and a normal acceleration of 0.48 g are encountered simultaneously just prior to booster separation, approximately 85 s after liftoff, with full propellant tanks. The rocket thrust is also a maximum at this time, 6.5 million lb. The lower surface of the fuselage must support a 2.0 psi aerodynamic load induced by the local flow conditions between the mated orbiter and booster which is based on an approximation using Space Shuttle criteria. The trajectory also imposes thermal loads on the structure which are discussed in a later section.

Design Criteria

The design criteria selected were:

1) 25-psi tank ullage pressure
2) Burst pressure of 2 times operating (ullage + hydrostatic head) pressure
3) Safety factor of 1.5 on nonpressure-induced loads
4) 1000-cycle design life with a scatter factor of 4
5) 3000°F operating temperature limit on ACC
6) 175°F operating temperature limit for cryogenic foam
7) 350°F operating temperature limit for aluminum
8) 32°F temperature limit for exterior surface to preclude ice/frost formation
9) Leak-free cryogenic tankage
10) 0.020-in.-thick aluminum minimum gage
11) 0.070-in.-thick ACC minimum gage
12) No pressure-stabilized design
13) Non-optimum factor of 1.2 on structural weights.

Bending Moments

Maximum bending moments are shown in Fig. 7 for the two nonintegral tanks of the near-art concept and the combined tanks of the advanced concept, along with the bending moment diagram of each airframe. Maximum bending occurs during ascent when the mated orbiter and fully fueled booster experience the 0.48-g normal acceleration. The maximum tank bending moment is about 43 million in.-lb in the near-art LOX tank and 100 million in.-lb in the advanced concept tank/thrust structure. Tank bending is higher in the advanced concept than in the near-art concept because the span between the tank supports is longer and the LH_2 tank is cantilevered. Moreover, for the advanced concept, the LOX tank transmits thrust to the forward hydrogen tank; thus, the compressive load intensity is the sum of that due to bending and that due to thrust. The location of the forward support in the aeroshell concept was selected to minimize bending moments consistent with maintaining a low relative deflection between the aeroshell and tank/thrust structure. Figure 8 shows the maximum aeroshell and tank deflections for the selected support locations. A maximum differential displacement of about 1.0 in. between the tank/thrust and aeroshell structure occurred at the forward end of the tank. Maximum bending moments for the near-art and advanced concepts fuselages, Fig. 7, are 174 and 159 million in.-lb, respectively.

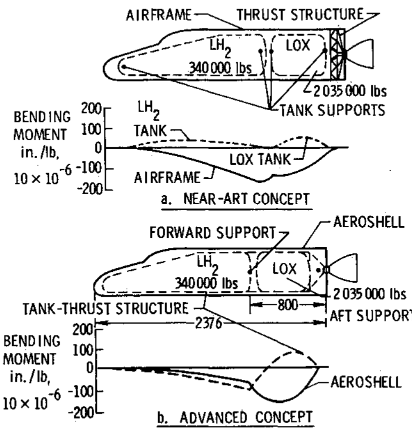

Fig. 7 Maximum airframe and tank bending moments for the near-art and advanced orbiter concepts (dimensions in in.).

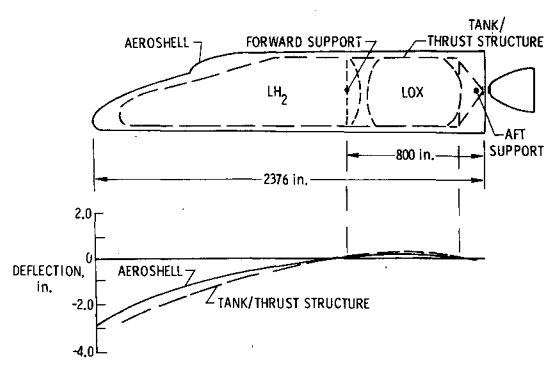

Fig. 8 Aeroshell and tank/thrust structure deflections in the advanced concept.

The maximum wing loading is also incurred during ascent. The fully fueled orbiter weight is 3 million lb, at this time. The 7,000-ft^2 wing has a 200-lb/ft^2 design load or a 113 million in.-lb moment at the wing root.

Cryogenic Tank Sizing

The cryogenic propellants, LOX at a temperature of $-297°F$ and LH_2 at a temperature of $-423°F$, must be contained in reusable, leak-tight, flight-weight tanks which are compatible with the propellants. The choice of materials is critical since many materials are LOX sensitive,[8] and/or are embrittled by hydrogen.[9] The low-temperature environment may also reduce ductility and fracture toughness to unacceptably low levels. The structural design goal of 1000 missions requires that the airframe and tanks let no cracks grow to a critical size during the period of inspection or the lifetime. For most structures (hydrocarbon fueled airplanes for instance) a crack may propagate through the thickness long before reaching critical size; however, for cryogenic tanks a crack through the thickness (a critical crack depth), while not a critical size structurally, can be catastrophic because leaking gaseous propellants are a fire/explosion hazard. Therefore, for reusable cryogenic tanks, the tank minimum wall thickness must exceed the critical crack depth. Based on these requirements, 2219 aluminum was selected for both the near-art and the advanced concept tanks. This alloy has moderately high strength coupled with low notch sensitivity at cryogenic temperature, and is compatable with both propellants and readily weldable.

Internal Pressure Loads

As shown by the dashed lines on Fig. 9, the cryogenic tank walls were primarily sized by internal pressure loads; however, portions of the tank were sized by buckling and fracture mechanics considerations. Although Fig. 9 is specifically for the aeroshell tank, the skin gages for pressure containment were similar for both concepts. Skin thicknesses of 0.10 to 0.42 in. were required from front to rear along the length of the LH_2 and LOX tanks to accommodate the local pressure which was the sum of the ullage and propellant head pressure during the 2.2-g axial acceleration.

Bending and Thrust Loads

The bending and thrust loads are of more concern for the advanced concept tank/thrust structure because the shorter near-art tanks are simply supported and tank bending moments are lower. For the advanced concept tank/thrust structure, the equivalent thickness ($\bar{t}$) of an optimized blade-stiffened skin, unpressurized tank required to resist the bending moment and thrust load, shown by the lower curves of Fig. 9, is much less than the thickness required for pressure containment. Furthermore, the unstiffened skin with pressure stabilization will not buckle; however, without pressure stabilization the unstiffened skin structure will buckle. Therefore, to prevent buckling, blade stiffeners and ring frames are required in the areas of high bending which are included in the $\bar{t}$ indicated by the solid curve in Fig. 9. Similarly, the near-art concept requires localized stiffening to resist the tank bending moment.

Tank Wall Cycle Life

Fracture life data for 2219-T87 aluminum[10] and the technique of Ref. 11 were used to calculate the number of cycles for a crack to propagate through the skin. The front end of the LH_2 tank is relatively thin (0.10-in. thick) when sized for pressure and requires no stiffening for bending (Fig. 9). The 0.10-in. thick aluminum tank skin, stressed to 29.3 ksi, does not meet the 4000-cycle goal with a 0.050-in. initial crack depth.[12] A minimum skin thickness of 0.15 in. is required to meet this goal. If an 0.015-in. crack could be detected, the 0.10-in. skin thickness exceeds the design life goal. Therefore, detection of small flaws or frequent inspections are required to meet the 1000-mission life requirement for a strength designed tank. For simplicity a skin thickness of 0.15 in. is used to satisfy the cycle life goal.

Airframe Structural Sizing

Fuselage Structures

The fuselage structures for both the near-art and advanced concepts were analyzed as 34-ft.-diam cylinders to simplify calculations for bending. However, the lower surface frames were analyzed as flat beams for the 2.0-psi pressure load. Because of the large fuselage diameter, bending produces a relatively low load intensity, N_x, of about 1330 and 1215 lb/in. in the near-art and advanced concepts, respectively. The fuselages are also loaded by the rocket thrust, which produces an additional N_x of 550 and 240 lb/in. in the near-art and advanced concepts, respectively. The load intensities occur at the point of maximum bending moment, thus producing design load intensities of 1880 and 1455 lb/in. for the near-art and advanced concepts, respectively. Corresponding load indices, N_x/RE, (including the factor of safety) where used to obtain the equivalent skin thicknesses, $\bar{t}$, using Fig. 10.[13]

For an unbuckled skin, the 2820 lb/in. maximum ultimate load intensity for the near-art concept requires a $\bar{t}$ of 0.12 in. for a Z-stiffened-skin aluminum structure (from Fig. 10). However, since the durable TPS is mechanically attached, on simple, slip-jointed supports at ring frames, ribs, and spars or stiffeners, the orbiter skin can be allowed to buckle. This permits a thinner $\bar{t}$ for the compression part of the fuselage which results in a significant reduction in fuselage mass. For the more efficient box stiffened skin which is allowed to buckle, the maximum fuselage skin $\bar{t}$ is 0.073 in.

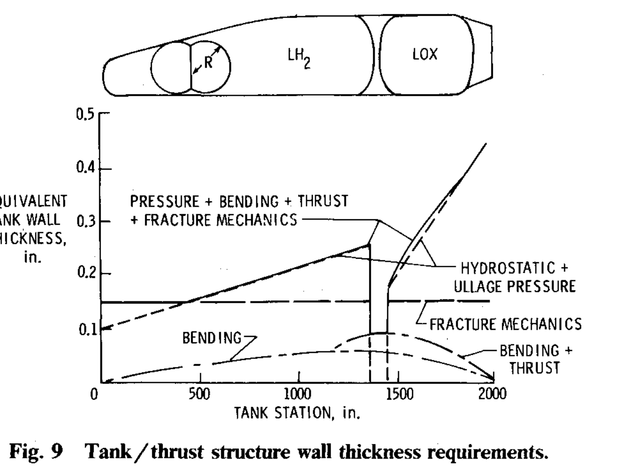

Fig. 9 Tank/thrust structure wall thickness requirements.

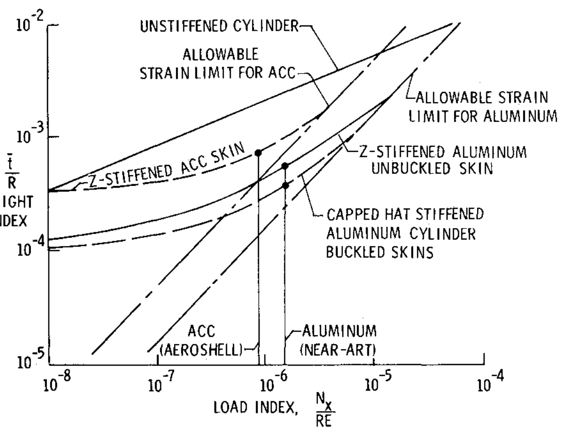

Fig. 10 Structural index curves for optimized cylindrical shells with ring frames.

The fuselage in the aeroshell orbiter has a lower ultimate load intensity (2180 lb/in. vs 2820 lb/in.) than the fuselage of the near-art concept and the ACC material has a slightly higher modulus of elasticity (12 msi vs. 10 msi, respectively). With skins and Z-stiffeners of 0.07 in., which is the minimum gage for the ACC material, and using Fig. 10 for a Z-stiffened cylinder, the ACC has a required $\bar{t}$ of 0.14 in. for the maximum design load index. The thick minimum gage for ACC inherently results in an unbuckled skin.

Another design consideration for both fuselage concepts is the relatively flat lower surface. This area must support a 2.0-psi aerodynamic load imposed by the local flow between the mated orbiter and booster. This load significantly increases the local weight of the fuselage ring frames because of the inefficiency of long straight frames for pressure loads.

Thrust Structures

The thrust structure of the near-art concept, Fig. 3, consists of a grid of beams about 34 ft high and 50 ft wide that transmit the rocket thrust to the airframe via long tapered longerons attached to the ends of each beam. The thrust beams are aluminum with boron-aluminum reinforcements on the inner and outer beam caps. The weight of this structure is 29,700 lb.

The thrust structure of the advanced concept, Fig. 5, consists of a ring and a conical thrust structure that connects to the rear of the LOX tank. The ring is about 25 ft in diameter and the relatively short conical structure carries the thrust directly to the tank/thrust structure. This structure is also aluminum with boron-aluminum reinforcements. This thrust distribution system is about 70% lighter than the near-art concept, because the near-art thrust structure spans the thrust by long beams to the fuselage structure.

Wing Structure

The maximum wing loading results in a 170 million in.-lb. ultimate moment at the wing root. Unlike the fuselage, the wing root structure is approximately equally loaded in both concepts. Based on a 12% wing thickness, the wing root ultimate load intensities are 9300 and 8900 lb/in. for the near-art and advanced concepts, respectively. The wing load intensity is higher in the near-art concept because the external TPS reduces the structural depth. The ultimate N_y varies linearly spanwise from a maximum at the root to zero at the tip and was used to size the wing structure.

The wing structures are similar to the fuselage wall structures shown in Figs. 4 and 6, except that the advanced concept requires no internal insulation or gas purge because there is no cryogenic tank in the wing. The lower wing surface is loaded primarily in tension and the required $\bar{t}$ is based on the strain limit for each material. For the compression surfaces, the wing skin thicknesses were determined using structural index curves for flat panels.[14] The higher elastic modulus of ACC yields a lower load index, 3.02×10^{-5} vs 3.82×10^{-5} for aluminum.

The maximum load index for the near-art aluminum wing root produces a $\bar{t}$ of 0.140 in. for a Z-stiffened panel 20 in. long. At this $\bar{t}$, the strain is less than the allowable strain limit, about 0.7%, for the aluminum in this compressive application. This indicates that the wing root is very close to a strain limit design and little weight reduction for a buckled skin is available in this area. However, the load index decreases with increasing wing span indicating a further weight reduction for the buckled wing skin, about 14% of the panel weight on the compression surface.

Compared with the aluminum wing structure, the ACC hot wing structure has a much lower allowable strain limit, 0.2%, which sizes the $\bar{t}$ for the ACC wing at 0.280 in. This is above the minimum gage for ACC and is substantially thicker than the aluminum wing skin. Also the ribs and spars in both concepts will be near minimum gage in each material which again imposes a penalty on the ACC structure.

Thermal Protection System Sizing

To determine the insulation requirements several locations along the fuselage length on both upper and lower surfaces were analyzed using the thermal model depicted in Fig. 11 and the transient heating code of Ref. 15. This code couples the aerodynamic heating with the radiation from the outer surface and with heat conduction into or out of the wall. The entry flight profile was used as input to the heating analysis.

Cryogenic Insulation

The cryogenic foam insulation requirements are the same for both the near-art and advanced concepts. Foam thicknesses were selected to prevent the hot face temperature from cooling below 32°F for altitudes below 65,000 ft where water vapor would condense and freeze. Foam thicknesses of 0.4 and 1.7 in., respectively, are required on the interior of the LH_2 tank and exterior of the LOX tank. The interior foam has a higher conductivity because it is permeated by the hydrogen, but the external aluminum tank wall provides a large thermal mass or heat sink which results in the lower insulation thickness. The exterior foam on the LOX tank has a lower conductivity but a very low thermal mass and, therefore, is thicker than the interior foam on the LH_2 tank.

Near-Art Concept External TPS

The near-art structure requires an external TPS to limit the aluminum surface to a 350°F maximum operating temperature during entry. The TPS concepts and their thermal properties were taken from Ref. 5. Figure 12 shows the temperature histories of the outer radiative surface, of the TPS, the aluminum airframe structure and the tank wall, 100 in. aft of the nose. At this location the tanks contain LH_2 and an internal cryogenic foam which cannot exceed 175°F. As shown, the radiation equilibrium temperatures are about 2400 and 750°F for the lower and upper surfaces, respectively. This condition requires a 2.9-in.-thick TPS for the lower surface weighing 2.0 lb/ft^2 and only a 0.25-in.-thick TPS on the upper surface weighing 0.4 lb/ft^2; an average TPS weight of

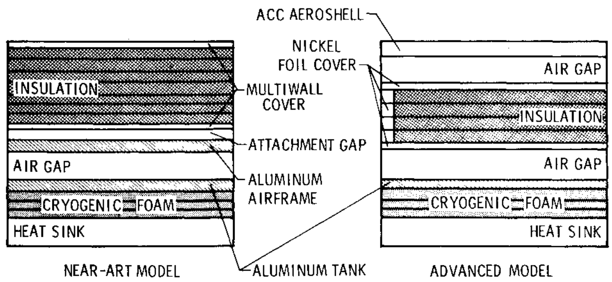

Fig. 11 Thermal models for near-art and advanced concepts.

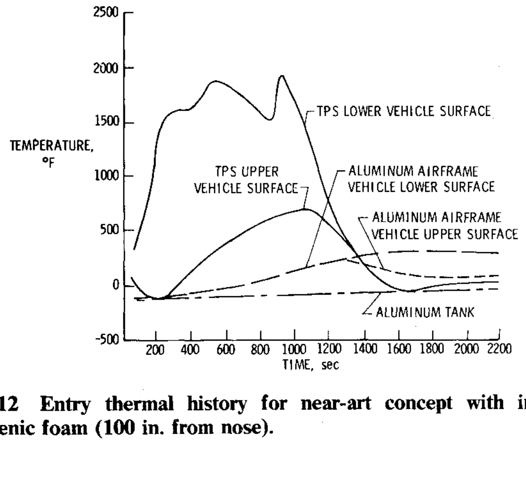

Fig. 12 Entry thermal history for near-art concept with internal cryogenic foam (100 in. from nose).

1.2 lb/ft^2 at a point 100 in. from the nose. The LOX tank area, 1200 inches aft of the nose, has higher radiation equilibrium temperatures, Fig. 13, because of transition to turbulent flow. Thus, the lower surface requires about 3.9 in.-thick TPS or 2.4 lb/ft^2. The upper surface remains at 0.25-in. thickness, 0.4 lb/ft^2, resulting in an average TPS in this region of 1.4 lb/ft^2. An average of these forward and aft TPS weights, 1.3 lb/ft^2, was used for the entire orbiter.

The aluminum airframe has insignificant temperature gradients and, therefore, thermal stresses were neglected.

Advanced Concept-Internal TPS

The insulation requirements for the aeroshell of the advanced concept were similarly evaluated. The ACC material can withstand the 2400°F maximum temperature and the ACC wing does not require insulation; however, the cryogenic foam must be maintained below 175°F. Thus, fibrous insulation blankets in foil-gage nickel-alloy containers are mounted inside the aeroshell fuselage. Figures 14 and 15 show the thermal histories for both forward and aft tank locations. The hot aeroshell requires thicker insulation than the externally insulated near-art concept, 3.5 in. forward and 6.0 in. aft, on the lower surface, because the aluminum structure of the near-art concept serves as a heat sink. The upper surface requires no insulation for the forward LH_2 tank, but does require 1.3 inches of insulation to protect the exterior foam on the LOX tank. The average weight of this internal insulation system is about 1.0 lb/ft^2 of the fuselage surface area.

The maximum temperature difference between the hot outer surface and the cooler inner frame caps during entry is about 2400°F as shown in Fig. 15. Because of the low coefficient of thermal expansion for ACC, the maximum thermal stress is less than 7000 psi, well below the 24,000 psi material strength.

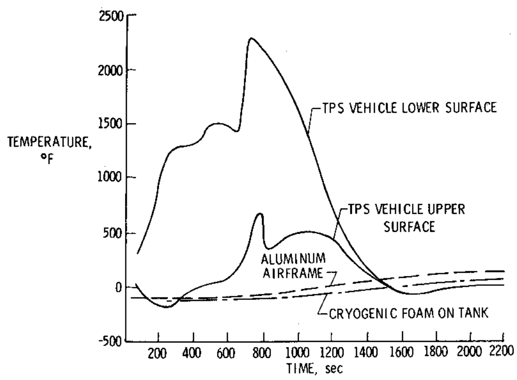

Fig. 13 Entry thermal history for near-art concept with external cryogenic foam (1200 in. from nose).

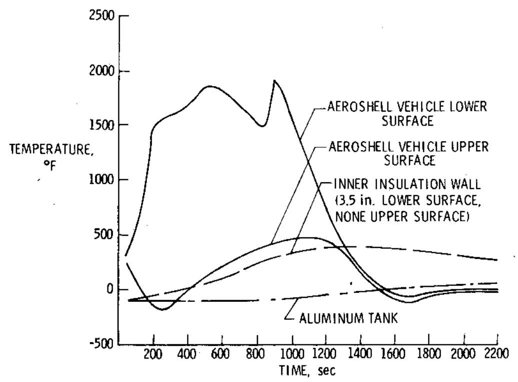

Fig. 14 Entry thermal history for advanced concept with internal cryogenic foam (100 in. from nose).

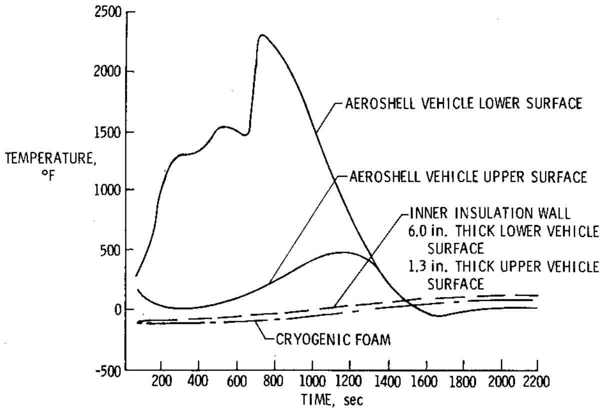

Fig. 15 Entry thermal history for advanced concept with external cryogenic foam (1200 in. from nose).

Concept Comparisons

Total dry weight of the advanced concept is about 13,100 lb and 6,400 lb less than the unbuckled and buckled skin near-art concepts, respectively, resulting in payload increases of corresponding amounts for the advanced concept. The advanced concept has a higher payload mass fraction, 2.30% of GLOW, compared with 2.04% and 2.16% for the near-art buckled and unbuckled skin concepts, respectively. Although not evaluated, a hybrid concept using a near-art insulated aluminum airframe for the aeroshell and the tank/thrust structure of the advanced concept is the least mass concept.

Cryogenic Tanks

The near-art and advanced concepts employ similar welded blade-stiffened aluminum cryogenic propellant tanks that are considered state of the art requiring minimal development. The welded joints provide leak-free containment and the 2219 aluminum is compatible with both the LH_2 and LOX. The tank structure, assuming an 0.050-in. initial flaw depth is shown to last the 1000-mission life. The basic structural concept concentrates the material in a single skin. Thus, only limited areas of the tank required additional material to meet the cycle life goal.

The foam insulation was sized to prevent ice formation during ascent and in conjunction with a dry air ground purge precludes air liquefaction on the tank walls. The foam insulation is similar to that used on the Saturn S-IVB vehicle and that proposed for hydrogen fueled aircraft. However, additional research is required to establish the expected foam life for the present application.

Unit weights for near-art and advanced concept tanks are 3.2 and 3.5 lb/ft^2, respectively. The additional weight in the advanced concept tank is required to carry the higher thrust and bending loads of the tank/thrust structure. Total tank weights are 62,800 for the near-art concept and 69,300 lbs for the advanced concept.

Fuselage Structures

The insulated aluminum fuselage in the near-art concept is also considered to be state of the art requiring minimal development. The metallic portion of the durable TPS proposed for the near-art structure represents a maturing technology.[16] Although this metallic TPS has not demonstrated the design life goal, unpublished test results of similar metallic TPS indicate that the 1000 mission life is attainable. The near-art and advanced concepts share the use of ACC which is in the embryonic stage of development (the near-art concept uses ACC TPS and the advanced concept uses ACC for the primary structure of the aeroshell). ACC is unique in that unlike metals it retains its mechanical properties at temperatures up to 3000°F. Thus, the use of ACC provides a significant overtemperature capability. Current life prediction[6] for

ACC, based on exposure tests, is 100 missions. The ACC material fabrication process is currently time intensive and restricts final component sizes. However, ACC is a rapidly developing material, and can be reasonably expected to have enhanced properties in time to support a FSTS development program. The present ACC exhibits almost three times the strength and one-half the oxidation mass loss[6] of its predecessor, reinforced carbon-carbon, which is currently used for the nose cap and leading edges of the space shuttle.

For the near-art concept the larger size of the durable TPS significantly reduces the number of tiles, by a factor of 4 relative to the current space shuttle which uses 6 × 6-in. tiles for its TPS. The mechanical attachment system eliminates the nonbuckled skin criteria currently used on the space shuttle. Allowing the skins to buckle between stringers reduces the airframe weight and consequently life cycle costs.

The ACC aeroshell of the advanced concept experiences a high aerodynamic heating environment combined with the air loads imposed by the lift forces during entry. This loading is relatively low compared with the load intensity of the tank/thrust structure and therefore the aeroshell is more suitable for a hot structure.[17] The monolithic ACC aeroshell, which is impervious to rain and weathering, provides a smoother aerodynamic surface than the near-art concept TPS.

The ACC aeroshell of the advanced concept which weighs 2.8 lb/ft^2 is lighter than the near-art concept fuselage which weighs 3.2 lb/ft^2 for a fuselage designed with nonbuckled skins and 3.0 lb/ft^2 for the fuselage with buckled skins. Furthermore, the ACC hot structure uses a lighter internal packaged fibrous insulation at 1.0 lb/ft^2 while the near-art concept uses 1.3 lb/ft^2 of external TPS. The total fuselage weight, including TPS, is 90,100 for the ACC aeroshell of the advanced concept, and 109,300 lb for the near-art concept with unbuckled skins, 103,900 for the near-art concept with buckled skins.

Thrust Structure

The thrust structure for the advanced concept is about one-third the weight of the near-art concept. The near-art concept thrust structure carries the thrust forces over the 34 ft depth and 50 ft width of the orbiter base and then transmits these loads into the fuselage. In the advanced concept, a more direct load path, the conical thrust adapter results in the weight savings. The advanced concept thrust structure weight includes a provision for the aft trunnion which supports the aeroshell.

Wing Structure

The wing structure is more highly loaded than the fuselage structure in both concepts. The wing structure of the near-art concept weighs 3.7 lb/ft^2, which is lighter than the 7.4 lb/ft^2 weight of the ACC wing of the advanced concept. The advanced concept wing is penalized by the low strength of ACC in the highly loaded wing skin panels and by the thicker minimum gage ACC material used on the lightly loaded webs of the wing ribs and spars. The total wing weight for the near-art concept including TPS is 5.1 lb/ft^2 or 40,100 lb compared to 59,000 lb for the ACC wing. A small weight decrease of about 0.1 lb/ft^2 can be attained if the wing compression surfaces are allowed to buckle in the near-art concept which will reduce the wing weight to 38,800 lb.

Conclusions

Two structural concepts, near-art and advanced, for a fully reusable FSTS orbiter were compared for their weight and ability to satisfy structural goals. The selected cryogenic propellant tanks for both concepts used welded, blade-stiffened aluminum skins for leak-free containment and compatibility with LOX and LH_2. These tanks are primarily sized by pressure, although some areas are sized by bending and fracture mechanics considerations. The tank concept is considered to be state-of-the-art, however, it requires a closed-cell foam insulation with a dry air purge to prevent air liquefaction and ice formation. The foam will require testing to verify its design life for FSTS application.

The near-art concept has nonintegral tanks suspended inside an insulated aluminum airframe and thrust structure. A durable external TPS is mechanically attached to the airframe allowing a buckled skin design. A buckled skin design is shown to be about 6000 lb lighter than a similar airframe using an unbuckled skin. The proposed durable TPS is considered to be a maturing technology and has tiles that are larger than those currently used on the Space Shuttle.

The advanced concept uses a novel structural arrangement consisting of a separate tank/thrust structure which supports a hot ACC aeroshell structure. The shorter thrust load path in this concept results in a lightly loaded aeroshell; this concept is 9000 lb lighter than the lightest near-art concept. The ACC is an embryonic material which has potential for improved oxidation life and strength. The ACC has not yet demonstrated the 1000-mission life; however, it has a smoother monolithic aerodynamic surface than the near-art tiles. Moreover, the ACC aeroshell is impervious to rain and weathering and requires no external TPS.

Although not specifically studied, a hybrid of the two concepts presented, consisting of an insulated aluminum aeroshell and tank/thrust structure, has a potential for lower mass and may be a more suitable concept for FSTS.

References

[1] Caluori, V.A., Conrad, R.T., and Jenkins, J.C., "Technology Requirements for Future Earth-to-Geosynchronous Orbit Transportation Systems, Volume II: Technical Results," NASA CR 3266, June 1980.

[2] Hepler, A.K. and Bangsund, E.T., "Technology Requirements for Advanced Earth Orbital Transportation Systems. Volume 2: Summary Report," NASA CR 2879, 1978.

[3] Jackson, L.R., Martin, J.A., and Small, W.J., "A Fully Reusable, Horizontal Takeoff Space Transport Concept with Two Small Turbojet Boosters," NASA TM 74087, Oct. 1977.

[4] Wilhite, A.W., "The Aerospace Vehicle Interactive Design System," NASA TM 81957, 1981.

[5] Hays, D., "An Assessment of Alternate TPS for the Space Shuttle Orbiter," NASA CR-165790, Feb. 1982.

[6] While, D.M., "Development of Advanced Carbon-Carbon (ACC) Composites, Volume II-ACC Cover Panel Feasibility Study," NASA CR-165842-2, Vol. 2, July 1982.

[7] Brauer, G.L., et al., "Program to Optimize Simulated Trajectories (POST), Volume 1-Formulation Manual," MCR-73-206, Oct. 1973.

[8] White, E.L. and Ward, J.J., "Ignition of Metals in Oxygen," Defense Metals Information Center Report 224, Feb. 1966.

[9] Chandler, W.T., "Hydrogen Embrittlement and Its Control in Hydrogen Fueled Engine Systems," NASA CP 2065, Sept. 1978, Part I, pp. 195-252.

[10] Witzell, W.E., "Evaluation of Mechanical Property Data on the 2219 Aluminum Alloy and Application of the Data to the Design of Liquid Hydrogen Tankage," NASA CR 145140, 1977.

[11] Newman, J.C. and Raju, I.S., "Analysis of Surface Cracks in Finite Plates Under Tension and Bending Loads," NASA TP 1578, Dec. 1979.

[12] Military Standard, Aircraft Structural Integrity Program, Airplane Requirements, MIL-STD-1530 (USAF), Sept. 1972.

[13] Shideler, J.L., Anderson, M.S., and Jackson, L.R., "Optimum Mass-Strength Analysis for Orthotropic Ring Stiffened Cylinders Under Axial Compression," NASA TN D 6772, July 1972.

[14] Jackson, L.R., Davis, J.G., and Wichorek, G.R., "Structural Concepts for Hydrogen Fueled Hypersonic Airplanes," NASA TN D 3162, 1966.

[15] Garrett, B., et al., "A General Transient Heat-Transfer Computer Program for Thermally Thick Walls," NASA TM X 2058, Aug. 1970.

[16] Shideler, J.L., et al., "Multiwall TPS—An Emerging Technology," NASA TM 83133, May 1981.

[17] Adelman, H.M., "Preliminary Design Procedure for Insulated Structures Subjected to Transient Heating," NASA TP 1534, Dec. 1979.